Energy, Mines and Resources Canada | Energie, Mines et Ressources Canada

CANMET

Canada Centre for Mineral and Energy Technology | Centre canadien de la technologie des minéraux et de l'énergie

^{220}Rn FLUX DENSITY MEASUREMENTS IN CANADIAN UNDERGROUND URANIUM MINES - PRACTICAL DIFFICULTIES

J. BIGU

ELLIOT LAKE LABORATORY

NOVEMBER 1989

To be submitted for publication in Radiation Protection Dosimetry

MINING RESEARCH LABORATORY
DIVISION REPORT MRL 90-48 (J)

^{220}Rn FLUX DENSITY MEASUREMENTS IN CANADIAN UNDERGROUND URANIUM MINES - PRACTICAL DIFFICULTIES

J. Bigu*

ABSTRACT

Radon-220 flux density measurements have been conducted in a number of locations in an underground uranium mine. Flux density measurements were estimated using the Two Point Measurement (2PM) method consisting of measuring ^{220}Rn progeny concentration levels at two different points a distance apart within a given section of the mine. Several mine (radiation) models were used for determining the flux density by the 2PM method. This method provides 'apparent' flux density values as opposed to flux density across the mine wall/air interface measured by 'fluxmeters'. Furthermore, the method is sensitive to sources and sinks of ^{220}Rn other than mine walls, as well as mining operations and mining activities of a diverse nature. The data reported here are subject to an undetermined degree of uncertainty because: a) ^{220}Rn progeny experimental data were used to calculate ^{220}Rn concentration values for the 2PM method (the latter measurements were far too time consuming and complex for mine personnel), and b) the theoretical approach (i.e., mine models) used is sensitive to the separation of the sampling stations, and of their distance to a mine origin or reference point. The data presented here represent the only ^{220}Rn flux density measurements available for Canadian underground uranium mines.

Key words: Flux density; Thoron; Thoron progeny; Uranium; Canadian underground uranium mines.

*Research Scientist and Radiation/Respirable Dust/Ventilation Project Leader, Elliot Lake Laboratory, CANMET, Energy, Mines and Resources Canada, P.O. Box 100, Elliot Lake, Ontario, Canada, P5A 2J6

INTRODUCTION

Accurate knowledge of thoron gas (^{220}Rn) emanation rates, k, from thorium (Th) bearing rock formations such as walls, roof and floor of certain underground (UG) uranium (U) mines permit the theoretical determination of ^{220}Rn and ^{220}Rn progeny levels in these mine atmospheres, as well as of other partially enclosed Th radioactive environments.

Theoretical prediction of radioactivity levels in working and living environments is of great practical interest from the occupational and health physics standpoints, providing, in addition, a substantial engineering aid in the planning and design of ventilation systems for the efficient control and reduction of airborne radioactivity.

Radon-220 flux density, J, across bulk matter/air interfaces of an air space of volume V partially or totally enclosed by Th-containing matter is another useful variable which is related to k provided the geometry of V, and hence, its total surface area, S, is known. In its simplest form k and J are related by the expression $k = JS$.

The ^{220}Rn flux density across bulk matter/air boundaries can be determined experimentally by means of a fluxmeter, an instrument which in its simplest version assumes the shape of an open-ended cylinder (can) or container which is sealed to, or driven into, the material surface of interest. The flux density, J, can be calculated from measurements of the growth of ^{220}Rn activity concentration, $[^{220}Rn]$, in the container versus time in a similar fashion to that used for estimating radon gas (^{222}Rn) flux density as discussed elsewhere[1-7]. However, because of the omnipresence of ^{222}Rn, reliable ^{220}Rn flux density measurements are very difficult to conduct, as shown below.

Alternatively, ^{220}Rn J measurements can be estimated by the two point measurement (2PM) method[8]. This method consists of taking air samples at two different points, i.e., stations or locations, a distance L apart, within

the volume of interest, and measuring [^{220}Rn] in the samples. From the geometry of the volume V and the values for [^{220}Rn] at the two sampling stations, the variable J can be calculated[8]. Again the same problem regarding the presence of ^{222}Rn in ^{220}Rn atmospheres is applicable to the 2PM method.

Depending on the geometry of V, physical and chemical characteristics of the bulk matter, e.g., rock formation, environmental variables, industrial operations and personnel activities, or the absence thereof, and airflow conditions, it can be shown that reliable measurements of J are considerably more difficult, complex and uncertain than might appear at first glance.

This paper presents data of ^{220}Rn flux density measurements in an underground U mine. Although the discussion presented here is specifically related to this particular U mine, similar arguments apply equally well to other partially or totally enclosed working or living environments.

THEORETICAL BACKGROUND

There is an important conceptual difference between the quantities determined by means of a fluxmeter and the 2PM method, namely:

1. The fluxmeter provides a measure of the amount of ^{220}Rn crossing the mine wall/air boundary of the opening covered by the fluxmeter's cross-sectional area. When the ^{220}Rn emanation rate is normalized to the total cross-sectional area of the fluxmeter, a measure of the ^{220}Rn flux density is obtained.
2. The 2PM method gives only 'apparent' values for the flux density as opposed to true emanation flux density from mine walls, as measured by the fluxmeter. (For simplicity, walls, ceiling and roof of mine openings will be referred to hereafter, as walls.) This is so because ^{220}Rn sources other than those from mine walls also contribute to the ^{220}Rn levels measured in the mine volume. These include discrete sources derived from

certain mining operations (e.g., leaching), and desorption of ^{220}Rn dissolved in mine water, to name but a few discrete sources of ^{220}Rn. Conversely, some ^{220}Rn sinks are also present such as large volumes of mine water which can dissolve ^{222}Rn and ^{220}Rn alike.

A relatively detailed discussion on the different mine factors that affect the measurement of J by the fluxmeter and the 2PM method has been given elsewhere[8,9], and will not be repeated here. However, some particular experimental difficulties specifically related to ^{220}Rn are discussed below.

The ^{220}Rn concentration from air samples withdrawn from the fluxmeter's volume cannot be measured easily because of the presence of ^{222}Rn in very substantial amounts. Time-delay techniques using scintillation cells in conjunction with gross alpha-particle counting are not sufficiently reliable because of the very short half-life of ^{220}Rn (~55 s) compared with the long half-life of ^{222}Rn (~3.8 d), and the relatively long half-life of ^{212}Pb (10.6 h) compared with the short half-life of the ^{222}Rn progeny, i.e., about 30 min. A more reliable method would require the use of alpha-particle spectrometry; however, this technique is much more complex analytically, it requires more sophisticated instrumentation, and is, in addition, more labour intensive than conventional gross alpha-particle counting. For these reasons alpha-particle spectrometry is not very practical, particularly when large numbers of samples need to be measured. Alpha-particle spectrometry of ^{220}Rn using silicon-barrier detectors and diffused-junction detectors has been used by the author elsewhere[10].

Flux density measurements of ^{220}Rn in the presence of ^{222}Rn can be made using activated charcoal in conjunction with a high purity Germanium detector for high gamma-ray resolution[11]. The possibility of using track etch detectors in complex $^{220}Rn/^{222}Rn$ mixtures has also been suggested.

A major difficulty associated with the determination of ^{220}Rn flux density by the 2PM method is a theoretical one. It arises with regard to the

range and applicability limit of the kinetic equations derived for the calculation of J. It can be shown[12] that for an underground (UG) U mine, the concentration of ^{220}Rn and its progeny increase from zero at t=0, for a given physical 'origin', to a maximum value when steady-state radioactivity conditions are reached at a distance from the origin for which the growth of radioactivity equals its rate of decay. The distance from the origin for which this condition occurs depends on airflow conditions, e.g., mine air residence time, and the particular radioisotope under consideration. Hence, it is to be theoretically expected that for distances from the origin equal to or greater than a given value, $[^{220}Rn]$ will not increase any more, and the method is no longer valid (see Appendix).

EXPERIMENTAL PROCEDURE AND CONSIDERATIONS

Although mostly ^{220}Rn progeny and ^{220}Rn flux density measurements are presented here, these measurements are only part of a major radiation and meteorological survey conducted at an underground U mine over a period of one year[8].

Underground measurements were divided into four main categories, namely, radioactivity measurements, meteorological measurements, physical and geometrical measurements of the mine and mine sections under consideration, and observations of interest regarding the physical appearance of working and inactive locations of the mine where measurements were made.

A wide variety of mine sampling sites was selected for sampling and monitoring purposes, as follows:

1. Main general areas (sections) of the mine;
2. Within each section a number of locations of interest were identified such as exhaust airways, travelways, shafts, main ramps, stopes and leaching areas; and
3. Within most locations, two or more sampling stations were selected.

The areas (sections), locations, and stations chosen were based on the following conditions of interest:

1. Physical characteristics of the rock formation, including the presence of fissures, cracks, faults, and water seepage.
2. Mine operations and personnel activities.
3. Ventilation conditions.
4. Mine water conditions.
5. Unusual, and other conditions.

The design of the mine sampling strategy was the responsibility of mine personnel who also conducted the mine sampling survey using grab-sampling methods. Some important limitations of the sampling strategy have been pointed out elsewhere[8,9].

Because of serious experimental difficulties and lack of adequate expertise and instrumentation, fluxmeters were not used by mine personnel for determining the ^{220}Rn flux density. As a result, attention was focused by mine personnel on the 2PM method as a means of obtaining ^{220}Rn flux density data. However, and for the same reasons indicated above, the ^{220}Rn concentration measurements necessary for this method were not made. Instead, ^{220}Rn progeny measurements, namely, ^{220}Rn progeny Working Level, WL(Tn), were carried out. The problem now was to find a satisfactory and reliable way to convert WL(Tn) data to ^{220}Rn activity concentration, $[^{220}Rn]$, data. It should be noted that the original ^{220}Rn progeny concentration data were calculated in terms of the Working Level, i.e., WL(Tn), for short. These data have subsequently been converted into the presently accepted SI units, namely, Potential Alpha Energy Concentration (PAEC) in $\mu J/m^3$. Because of this, the reader should be aware that data are often given in both units and that frequent mention of both is made throughout the text. This has been done for the benefit of readers who are not completely familiar with both systems of units.

In order to accomplish the above conversion, a series of concurrent (parallel), side by side, measurements of [^{220}Rn] and WL(Tn) were conducted by the author at several mine locations under different airflow conditions. Data on the ratio WL(Tn)/[^{220}Rn] were gathered and analyzed. It was found that this ratio was reasonably constant, within certain limits, thereby providing an approximate means to arrive at [^{220}Rn] values from WL(Tn) measurements (see Appendix).

Radon-220 activity concentration measurements were conducted by the two-filter method[13,14]. Radon-220 progeny measurements, i.e., WL(Tn), were made using a modified version of the Rock method [15,16].

The reader should be aware of the approximate nature of the experimental/theoretical procedure used in this paper to obtain J, and hence to find a solution to a difficult practical problem. Notwithstanding the above, however, the results presented here using the 2PM method, and several mine models (see Appendix), represent the only set of data available for the ^{220}Rn flux density for Canadian U mines.

EXPERIMENTAL RESULTS AND DISCUSSION

Some data of interest in the context of this paper are shown in Figures 1 to 5 and Tables 1 to 4.

Figure 1 shows ^{220}Rn progeny concentration histograms, in terms of WL(Tn) and PAEC, for several UG locations. As expected, the lowest values for PAEC are found in airways, i.e., theoretically, fresh air intakes, although in practice significant air recirculation may take place because of leakage paths in the ventilation network. Similarly, the highest values for PAEC are mostly found, for obvious reasons, in exhaust airways. As previously indicated, ^{220}Rn progeny concentration levels depend on UG airflow conditions, environmental factors such as barometric pressure and aerosol concentration, the presence (or absence) of mining operations, the circulation of vehicles

and machinery, worker traffic, and the physical conditions and geometry of the mine locations where measurements are conducted, e.g., water drainage and water seepage through mine walls and roof.

The data shown in Figure 1 are representative of average UG conditions. The broad range of values measured for PAEC at each UG location is related to the UG variable conditions indicated above, e.g., airflow and environmental conditions, mining operations, and the like.

Figure 2 shows the (normalized) ^{220}Rn progeny concentration frequency histogram for all UG locations where measurements were carried out for a period of one year. The data of Figure 2 are based on data shown in Figure 1. Figure 2 shows that most values were in the approximate range 1 $\mu J/m^3$ to ~4 $\mu J/m^3$.

Figure 3 shows a (normalized) frequency histogram of the ^{220}Rn concentration calculated from measurements of PAEC or WL(Tn) as previously discussed. The relationship between the ^{220}Rn activity concentration, $[^{220}Rn]$, and WL(Tn) obtained was (see Table 1): $[^{220}Rn] \sim 5 \times 10^2$ WL(Tn), where $[^{220}Rn]$ is given in pCi/L. The relationship when $[^{220}Rn]$ is expressed in Bq/m^3, and the ^{220}Rn progeny concentration (PAEC) is given in $\mu J/m^3$ is: $[^{220}Rn] \sim 921.31$ (PAEC). (The reader should be aware that the above relationships are only applicable to the particular UG U-mine where the general radiation survey program was carried out, and under the range of airflow conditions investigated.) Figure 3 shows a wide distribution for the values of $[^{220}Rn]$, i.e., from <74 Bq/m^3 (2 pCi/L) to >3.33 x 10^3 Bq/m^3 (90 pCi/L). This is clearly indicative of the wide range of airflow conditions, and the wide variety of mining locations and field conditions prevailing in the UG mine investigated.

Figure 4 shows the important ratio of ^{220}Rn progeny concentration to ^{222}Rn progeny concentration, namely, PAEC(Tn)/PAEC(Rn). The PAECs ratio is given as a (normalized) frequency histogram. This ratio is important because

it is very sensitive to airflow conditions and, hence, can be used as an index of ventilation performance as discussed elsewhere[12]. The wide range of values measured for PAEC(Tn)/PAEC(Rn) confirms the wide range of airflow conditions and other conditions alluded to above. Figure 5 shows the ^{220}Rn flux density frequency histogram for three areas of the mine (combined) calculated according to the MTMV mine model (see Appendix), and the relationship between [^{220}Rn] and PAEC indicated above.

Table 1 shows measurements of [^{220}Rn], and ^{220}Rn progeny concentration (as PAEC, and also for reference purposes as WL(Tn)) conducted at several mine stations using the two filter tube (2FT) method, and a 'modified' ^{220}Rn progeny method developed by the author[16]. To the knowledge of the author, these represent the first direct measurements of ^{220}Rn activity concentration in Canadian UG U-mines. The Table shows parallel measurements of [^{220}Rn] and PAEC(Tn) and WL(Tn) for several sampling stations at two mine locations, namely, an exhaust airway, and a travelway. Also shown in Table 1 are airflow measurements, and the ratios WL(Tn)/[^{220}Rn], where [^{220}Rn] is in pCi/L, and the ratio PAEC(Tn)/[^{220}Rn], where [^{220}Rn] is in Bq/m^3.

Under ideal (theoretical) conditions, the variables [^{220}Rn] and PAEC(Tn) should be inversely related to UG airflow rate conditions, i.e., Q. However, the data of Table 1 do not show this clear relationship in spite of the great degree of care taken in conducting the field measurements. This departure from theoretical expectations is no doubt caused by the great complexity of the mining environment in part arising from a diversity of simultaneous mining operations and human activities, as previously indicated.

The data of Table 1 were primarily collected in order to investigate whether a value for the ratio PAEC(Tn)/[^{220}Rn] could be obtained that was sufficiently reliable, i.e., constant, for practical applications. As discussed above, this ratio could then be applied to calculate [^{220}Rn] from measurements of PAEC(Tn) or WL(Tn). The values of [^{220}Rn] so obtained could

then, in turn, be used to calculate ^{220}Rn flux density measurements by the 2PM method. Although the values given in Table 1 for the ratios WL(Tn)/[^{220}Rn] and PAEC(Tn)/[^{220}Rn] varied significantly, their mean values, and standard deviation, namely, (2.11 $\pm$ 0.7) x 10^{-3} WL/pCiL^{-1} and (1.18 $\pm$ 0.38) x 10^{-3} μJ/Bq, respectively, are considered reasonably representative of UG conditions in this U-mine, particularly when it is realized that measurements were conducted over a wide range of airflow conditions, i.e., ~12 m^3/s to ~67 m^3/s.

It should also be noted that because of the inherent errors associated with the experimental determination of the above ratios, the accuracy of [^{220}Rn] calculated from measurements of WL(Tn) or PAEC(Tn) cannot be expected to be better than within 50% to 100% of their 'true' values when direct determinations of [^{220}Rn] are conducted. From the data in Table 1 one may summarize the approximate calculation of [^{220}Rn] as follows:

1. if [^{220}Rn] is in pCi/L: [^{220}Rn] ~2.0×10^{-3} WL(Tn),
2. if [^{220}Rn] is in Bq/m^3: [^{220}Rn] ~1.2×10^{-3} PAEC(Tn).

Table 2 shows the effect of mining operations or human activities (e.g., vehicle traffic) for a few underground locations for which airflow conditions remained constant throughout. In general, the main conclusion that can be drawn from this limited set of data is that an increase in ^{220}Rn progeny activity was observed when:

1. traffic of vehicles and personnel occured relative to non-traffic conditions;
2. any mining activity or operation was initiated relative to non-traffic, non-operation condition; and
3. slushing operations took place relative to drilling operations.

Table 3 shows ^{220}Rn flux density data calculated according to the MTEMM and MTMV models (see Appendix), and ^{220}Rn progeny concentration data, WL(Tn) and PAEC(Tn), for a selected number of pairs of UG mine sampling stations where measurements were conducted. Also shown in the Table are the air

residence time (RT), the air linear velocity (v), and the distance between pairs of sampling stations (L).

The data for J(^{220}Rn) calculated according to the above models are in visible disagreement with each other. Data calculated according to the Thomas-Epps Mine Model (TEMM), and other models, have not been included in this paper because they ignore the radioactive decay of the parent radioactive gas, i.e., ^{220}Rn, during its transit (flight) time between sampling stations. Although this approximation is acceptable for ^{222}Rn because its radioactive half-life (~3.8 d) is so long compared to its residence time (RT = L/v) between sampling stations that radioactive decay effects can safely be ignored, for ^{220}Rn, radioactive decay effects cannot be ignored because of its short half-life (~55 s).

The disagreement between the values for J(^{220}Rn) predicted by the MTEMM and MTMV models, and most certainly, between each of these models and 'true' values for the flux density may arise because of the following. Field measurements at each pair of sampling stations, say A and B, were not carried out at the proper time relative to one another, namely, measurements at the downstream location (B) should be carried out at a time $t = t_o + (L/v)$, where t_o is the time at which measurements are conducted at the upstream location (A). This experimental procedure should be followed to ensure that measurements at B are related to the same 'volume front' as that measured at A.

Under true (ideal) steady-state and constant conditions, and in the absence of mining operations and other mining activities, the condition $t = t_o + (L/v)$ is not so important. However, these conditions and requirements are rarely met in practice. Changes in airflow conditions, and the presence of mining operations and personnel activities can greatly affect the spatio-temporal radioactive levels in a given section of the mine. Mining operations are discrete in time and space, i.e., they are irregularly restricted or confined to a section of the mine, usually smaller than the volume (V)

enclosed by L. Personnel activities, such as vehicle traffic, and the like, are also discrete and highly irregular or intermittent in nature.

The factors alluded to above explain why radioactivity levels at Station B may be lower than levels at Station A and other hosts of experimental observations. It is not the intention of this paper to enumerate all the different factors that may affect radioactivity concentration levels in UG mine environments. This will be immediately obvious to the experienced reader.

Because of the basic assumptions made for each model, it is considered here that, in general, the MTMV model provides a better description of underground conditions than other mine (radiation) models. This is also partly supported by the absence of negative values for $J(^{220}Rn)$ in Table 3 for the MTMV.

Table 4 shows data for the flux density ratio $J(^{220}Rn)/J(^{222}Rn)$ for several mine locations. Also shown in the Table are the air residence times corresponding to these locations. It can be shown that for a weight ratio of ^{238}U to ^{232}Th equal to unity (the actual weight ratio for the mine where measurements were made is in the approximate range 1 to 4), the ^{220}Rn to ^{222}Rn flux ratio at the air/mine wall interface is about 1/240 ~4 x 10^{-3} (12). This value is considerably smaller than the values reported in Table 4 which range from ~1 to ~63. However, it should be noted that the model used for the above calculation of the flux density ratio is a one-dimensional one. Furthermore, no transport phenomena were taken into account, and the physico-chemical properties and conditions of the rock formation were not considered.

It remains to be seen whether the above departure from ideal conditions and the simplification made in the models used are sufficient to account for the great difference observed between experimental and theoretical data. These differences have to do, no doubt, with the great uncertainty in calculating $Jn(^{220}Rn)$ by the 2PM method based on WL(Tn), or PAEC(Tn),

measurements instead of the much more experimentally complex [^{220}Rn] measurements, by the rather arbitrary choice (although subject to practical constraints) by mine personnel of the distance (L) between sampling stations (see Appendix), and by the theoretical limitations, and assumptions made in the theoretical methods used.

CONCLUSIONS

Because of man-power and instrumentation considerations, practical and economical constraints, and experimental difficulties by mine staff, a simplified approach for determining ^{220}Rn flux density from ^{220}Rn progeny data has been used. The method reported here makes use of a theoretical approach, namely, the use of mine (radiation) models in conjunction with experimental data for ^{220}Rn progeny. The latter measurements of WL(Tn) or PAEC(Tn) were made by mine personnel, instead of the more time consuming, delicate, and prohibitively complex ^{220}Rn activity concentration levels. Hence, the data presented here are somewhat uncertain because of the following:

1. Great care must be exercised when using the 2PM method. Hence, the sampling stations should be chosen so as to maximize the accuracy of the theoretical approach, as indicated in the Appendix. For this reason, L, the distance between pairs of stations, and their distance to an 'accepted' mine origin are very important.
2. The values for the ^{220}Rn activity concentrations are subject to an unknown degree of uncertainty because they have been calculated from WL(Tn) or PAEC(Tn) measurements, as previously discussed.

No direct ^{220}Rn flux density measurements using fluxmeters at the mine wall/air interface were made, for reasons previously discussed, to compare and complement 'apparent' ^{220}Rn flux density measurements by the 2PM method with wall flux data.

Although much can be done to improve the accuracy of the data presented

here, this can only be done at an enormous expense in time, instrumentation, and labour. The data reported here represent the only source of $J(^{220}Rn)$ data for Canadian UG U-mines.

ACKNOWLEDGEMENTS

Most of the data presented here were collected at Denison Mines Ltd. (Elliot Lake, Ontario, Canada) by mine personnel. The author is particularly grateful to J.L. Chakravatti for many helpful technical discussions regarding the data, and for kindly agreeing to the publication of these data. The author is also grateful to D. Schryer for making the data available and for facilitating some underground measurements. Finally, thanks are also extended to C. Seeber for his assistance in reformatting the data and clarifying many important points.

REFERENCES

1. Kraner, H.W., Schroeder, G.L. and Evans, R.D. Measurements of Effects of Atmospheric Variables on Radon-222 Flux and Soil Gas Concentration. In: The Natural Radiation Environment. Chicago (IL), University of Chicago Press, 191-215 (1964).

2. Wilkening, M.H., Clements, W.E. and Stanley, D. Radon-222 Flux Measurements in Widely Separated Regions. In: The Natural Radiation Environment II. Springfield (VA), National Technical Information Service, 717-730 (1972).

3. Countess, R.J. ^{222}Rn Flux Measurements with a Charcoal Canister. Health Phys. 31, 455-456 (1976).

4. Fleischer, R.L. Radon Flux From the Earth: Methods of Measurement by the Nuclear Track Technique. Corp. Res. and Develop., General Electric Co., Schenectady (New York), Rep. 80 CR D070 (1980).

5 Schiager, K.J. Radon Flux Measurements: Classical Methods; ALARA Inc., Fort Collins, CO (1980).

6. Bigu, J. Use of an Automated Fluxmeter Employing Solid-State Diffused-Junction Alpha-Detectors and a Meteorological Package to Determine Surface Radon Flux. IEEE Trans. Nucl. Sci. NS-31(6), 1599-1606 (1984).

7. Kearney, P.D. and Krueger D.A. Radon-222 Flux Density Measurements Using an Accumulator: an Alternative Technique. Health Phys. 53, 525-526 (1987).

8. Bigu, J. An Evaluation of Radiation and Meteorological Conditions in an Underground Uranium Mine. Mining Research Laboratory (CANMET, Energy, Mines and Resources Canada, Ottawa), Division Report MRL 89-36(TR) (1988).

9. Bigu, J. Practical Difficulties in Determining ^{222}Rn Flux Density in Underground U Mines. Mining Research Laboratory (CANMET, Energy, Mines and Resources Canada, Ottawa) Division Report MRL 89- (J) (1989).

10. Bigu, J. A Method for Measuring Thoron and Radon Gas Concentrations Using Solid-State Alpha-Particle Detectors. Appl. Radiat. Isot. (Int. J. Radiat. Appl. Instrum. Part A) 37, 567-573 (1986).

11. Bigu, J. Radon-220 Determination Using Activated C and a High-Purity Ge Detector. Health Phys. 51, 534-538 (1986).

12. Bigu, J. Theoretical Models for Determining ^{222}Rn and ^{220}Rn Progeny Levels in Canadian Underground Uranium Mines - A Comparison with Experimental Data. Health Phys. 48, 371-399 (1985).

13. Thomas, J.W. Thoron Determination by the Two-Filter Method. Health and Safety Laboratory (HASL) Technical Memorandum 71-1, New York, NY 10014 (1971).

14. Mayya, Y.S. and Kotrappa, P. Modified Double Filter Method for the Measurement of Radon and Thoron in Air. Ann. Occup. Hyg. 21, 169-176 (1978).

15. Rock, R.L. Sampling Mine Atmospheres for Potential Alpha-Energy Due to Presence of Radon (Thoron) Daughters. U.S. Dept. of the Interior Information Report IR 1015 (U.S. Bureau of Mines, Denver, CO) (1975).

16. Bigu, J. and Grenier, M. Thoron Daughter Working Level Measurements by One and Two Gross Alpha-Count Methods. Nucl. Instr. and Methods in Phys. Res. 225, 385-398 (1984).

Table 1 - Thoron and thoron progeny concentration for two underground mine locations and several sampling stations.

Date YY/MM/DD	Location	[^{220}Rn] pCi/L(Bq/m^3)	[^{220}Rn Progeny]$^+$ WL(μJ/m^3)	Q m^3/s	Remarks	WL(Tn)* / [^{220}Rn]	PAEC(Tn)** / [^{220}Rn]
87/11/16	Exhaust	194.4 (7193)	0.462 (9.61)	-		2.38×10^{-3}	1.34×10^{-3}
	airway	192.1 (7108)	0.454 (9.44)	-		2.36	1.33
		203.6 (7533)	0.482(10.03)	-		2.37	1.33
87/11/19	Exhaust	217.1 (8033)	0.473 (9.84)	-		2.18	1.22
	airway	222.4 (8229)	0.490(10.19)	-		2.20	1.24
		202.9 (7507)	0.504(10.48)	-		2.48	1.40
87/12/17	Exhaust	209.4 (7748)	0.458 (9.53)	-		2.19	1.23
	airway	236.7 (8758)	0.458 (9.53)	-		1.93	1.09
		225.4 (8340)	0.455 (9.46)	-		2.02	1.13
87/11/04	Travelway	82.5 (3053)	0.081 (1.68)	37.8		~1.00	0.55
		67.1 (2483)	0.074 (1.54)	37.8		1.10	0.62
		75.1 (2779)	0.091 (1.89)	37.8		1.20	0.68
87/12/30	Travelway	39.1 (1447)	0.101 (2.10)	23.6		2.58	1.45
		32.2 (1191)	0.110 (2.29)	23.6		3.40	1.92
		28.5 (1055)	0.106 (2.20)	23.6		3.70	2.08
88/01/07	Travelway	43.8 (1621)	0.063 (1.31)	20.3		1.44	0.81
		42.0 (1554)	0.065 (1.35)	20.3		1.55	0.87
		37.5 (1388)	0.061 (1.27)	20.3		1.60	0.91
88/01/26	Exhaust	191.8 (7097)	0.439 (9.13)	63.5	A	2.29	1.29
	airway	251.6 (9309)	0.482(10.03)	62.7	B	1.92	1.08
		197.2 (7296)	0.437 (9.09)	64.5	A	2.22	1.24
		167.0 (6179)	0.459 (9.54)	58.8	B	2.75	1.54
88/01/27	Exhaust	230.6 (8532)	0.419 (8.72)	62.5	A	1.82	1.02
	airway	245.2 (9072)	0.456 (9.48)	63.7	B	1.86	1.04
		217.7 (8055)	0.428 (8.90)	66.4	A	1.97	1.10
		163.0 (6031)	0.444 (9.23)	60.7	B	2.72	1.53
88/01/28	Travelway	65.4 (2420)	0.083 (1.73)	17.0	C	1.27	0.71
		224.0 ?	0.095 (1.97)	16.3	D	-	-
		51.8 (1917)	0.074 (1.54)	14.5	C	1.43	0.80
		59.7 (2209)	0.089 (1.85)	17.1	D	1.49	0.84
88/01/29	Travelway	70.4 (2605)	0.089 (1.85)	17.0	C	1.26	0.71
		45.7 (1691)	0.132 (2.75)	14.8	D	2.89	1.63
		46.7 (1728)	0.110 (2.29)	12.5	C	2.35	1.32
		43.0 (1591)	0.152 (3.16)	14.4	D	3.53	1.99
				Average:		2.108×10^{-3} $\pm0.705\times10^{-3}$	1.18×10^{-3} $\pm0.38\times10^{-3}$

Note: The letters A, B, C and D refer to sampling stations.
*[^{220}Rn] in pCi/L,
**[^{220}Rn] in Bq/m^3.
$^+$square brackets denote concentration.

Table 2 - Effect of mining operations or activities on airborne radioactivity for several underground locations.

Location	Operations	ΔWL(Tn) or ΔPAEC(Tn) %
Jackleg stope	Drilling, Slushing	31
Travelway	No traffic > Setting up	90
Jackleg stope	No traffic > Drilling	136
Jackleg stope	No traffic > Setting up	?
Exhaust airway	No traffic > Traffic	104
Crusher decline	No traffic > Traffic	-21
Travelway	No traffic > Traffic	-19

Note: the symbol Δ is used to indicate increment.

Table 3 - ^{220}Rn flux density, ^{220}Rn progeny and airflow conditions data in an underground uranium mine.

Q (m^3/s)	RT (s)	$WL(Tn)_2$	$WL(Tn)_1$	J(MTEMM) Bq/m^2s	J(MTMV) Bq/m^2s	v m/s	L m
188.77	193.64	0.01	0.00	5.73	5.73	4.20	812.5
206.30	137.37	0.01	0.02	-7.53	6.57	3.55	487.8
212.36	133.45	0.02	0.01	7.64	14.76	3.66	487.8
15.84	513.46	0.03	0.02	3.46	10.37	0.61	312.5
18.88	430.78	0.02	0.01	3.55	7.09	0.73	312.5
24.07	337.90	0.01	0.00	3.71	3.71	0.92	312.5
19.89	67.02	0.34	0.28	35.84	176.85	1.27	85.4
24.24	54.99	0.19	0.23	-27.56	101.94	1.55	85.4
17.69	75.36	0.24	0.25	-5.51	112.87	1.13	85.4
6.13	1057.42	0.58	0.31	79.70	171.21	0.28	293.6
4.96	1306.85	0.28	0.26	5.83	81.56	0.22	293.6
1.89	3429.61	0.25	0.27	-5.62	70.26	0.09	293.6
54.73	20.18	0.09	0.08	15.25	102.55	3.81	76.8
67.40	16.39	0.05	0.07	-36.85	53.61	4.69	76.8
22.79	34.62	0.03	0.02	9.58	24.20	1.58	54.6
21.71	14.79	0.08	0.03	59.70	84.61	3.69	54.6
25.77	18.16	0.11	0.05	101.49	161.36	1.76	32.0
23.41	19.99	0.02	0.02	0.00	22.17	1.60	32.0
23.50	19.91	0.04	0.04	0.00	44.47	1.61	32.0
25.77	12.46	0.09	0.11	-47.28	131.10	1.81	22.6
23.41	13.71	0.05	0.02	64.84	94.70	1.65	22.6
23.50	13.66	0.08	0.04	86.76	146.69	1.65	22.6
23.50	28.65	0.07	0.08	-14.21	70.43	0.99	28.3
9.44	231.06	0.10	0.08	6.57	32.33	0.50	115.5
9.56	228.16	0.05	0.03	6.60	16.29	0.51	115.5
8.73	249.85	0.05	0.04	3.21	15.84	0.46	115.5
4.72	462.12	0.05	0.02	8.44	14.07	0.25	115.5
13.57	116.13	0.06	0.04	8.32	23.55	0.87	101.2
19.23	448.11	0.03	0.04	-3.04	9.10	0.86	385.4
18.16	86.78	0.07	0.03	9.33	15.47	4.44	385.4
16.75	220.85	0.06	0.06	0.00	21.04	0.75	164.6
8.97	412.40	0.05	0.03	6.17	15.41	0.40	164.6
4.11	475.14	0.51	0.12	162.30	212.19	0.11	52.7
4.11	475.14	0.46	0.19	112.36	191.36	0.11	52.7

Cont.

Q (m^3/s)	RT (s)	$WL(Tn)_2$	$WL(Tn)_1$	J(MTEMM) Bq/m^2s	J(MTMV) Bq/m^2s	v m/s	L m
4.11	435.14	0.51	0.40	46.95	217.42	0.11	47.3
4.11	435.14	0.46	0.43	12.80	196.07	0.11	47.3
4.72	1241.77	0.77	0.62	60.83	312.24	0.11	137.5
4.11	1426.07	0.19	0.26	-28.17	76.45	0.10	137.5
4.11	356.19	0.40	0.30	44.97	179.36	0.11	37.5
4.11	356.19	0.43	0.26	76.46	192.93	0.11	37.5
0.46	860.51	0.98	0.16	213.36	254.99	0.02	18.6
0.46	1215.36	0.96	0.48	117.61	235.23	0.02	29.9
17.59	28.15	0.11	0.08	35.66	106.30	1.12	31.4
17.59	66.20	0.11	0.08	18.44	59.83	1.08	71.3
15.80	73.69	0.03	0.03	0.00	14.66	0.97	71.3
15.80	31.34	0.14	0.03	119.32	143.82	1.00	31.4
15.80	42.36	0.03	0.14	-95.72	-0.05	0.94	39.9
47.19	38.55	0.08	0.10	-19.07	54.80	2.74	105.8
47.19	64.38	0.11	0.10	6.33	59.33	2.86	183.8
47.19	25.82	0.11	0.08	38.34	113.50	3.02	78.0
50.97	12.60	0.13	0.12	21.78	201.20	4.09	51.5
47.19	13.61	0.11	0.08	60.80	172.77	3.79	51.5
4.78	84.42	0.09	0.09	0.00	36.62	0.36	30.5
61.35	102.14	0.06	0.06	0.00	27.02	2.87	293.3
37.75	179.97	0.07	0.08	-3.94	26.43	1.69	304.3
61.35	40.66	0.10	0.06	39.51	85.78	2.74	111.6
61.35	85.62	0.11	0.08	18.04	60.19	2.48	212.5
61.35	44.63	0.11	0.10	9.95	88.72	2.26	100.9
31.89	211.26	0.06	0.05	3.78	22.23	1.37	289.6
31.89	191.45	0.07	0.04	11.80	27.03	1.39	266.8
39.01	124.25	0.05	0.06	-5.08	23.11	1.37	170.7
35.51	242.12	0.03	0.04	-5.25	15.41	0.41	98.2
37.16	231.37	0.11	0.03	42.63	58.30	0.42	98.2

Cont.

Q (m^3/s)	RT (s)	$WL(Tn)_2$	$WL(Tn)_1$	J(MTEMM) Bq/m^2s	J(MTMV) Bq/m^2s	v m/s	L m
35.51	263.26	0.04	0.04	0.00	19.74	0.48	125.6
37.16	251.57	0.10	0.03	35.45	50.42	0.50	125.6
39.01	261.67	0.13	0.06	28.66	52.19	1.22	318.6
35.51	287.47	0.08	0.04	15.98	31.81	1.11	318.6
37.16	274.70	0.11	0.03	32.33	44.32	1.16	318.6
39.01	136.07	0.13	0.05	44.97	71.25	1.09	147.9
35.51	23.22	0.04	0.03	18.88	60.02	1.18	27.4
37.16	22.19	0.10	0.11	-19.66	136.58	1.24	27.4
35.51	42.79	0.08	0.03	56.76	83.54	1.16	49.7
37.16	40.89	0.11	0.11	0.00	101.16	1.22	49.7
35.51	19.57	0.08	0.04	89.23	152.87	1.14	22.3
37.16	18.71	0.11	0.10	23.24	188.26	1.19	22.3
13.21	238.95	0.15	0.16	-4.87	71.62	0.29	68.6
13.63	189.31	0.12	0.12	0.00	56.47	0.31	59.4
16.52	213.08	0.12	0.15	-17.39	67.42	0.23	48.8
13.21	266.47	0.10	0.13	-16.25	53.29	0.18	48.8
13.52	260.36	0.14	0.16	-10.90	75.14	0.19	48.8
33.51	61.39	0.07	0.07	0.00	48.74	0.89	54.9
33.51	90.71	0.17	0.09	46.84	93.42	1.18	106.7
35.92	41.70	0.13	0.11	22.95	121.87	0.98	40.8
34.92	42.90	0.10	0.09	11.22	90.68	0.95	40.8
35.92	274.12	0.15	0.11	18.03	67.06	0.60	164.0
33.51	257.44	0.25	0.07	70.86	98.04	1.08	279.0
13.21	81.79	0.14	0.14	0.00	69.09	0.63	51.8
12.74	84.81	0.15	0.13	11.09	74.12	0.61	51.8
33.51	192.83	0.25	0.07	76.21	104.91	1.16	224.1
46.25	139.71	0.36	0.14	106.77	170.49	1.60	224.1
35.92	143.62	0.15	0.13	10.81	76.89	0.86	123.2
9.67	529.25	0.20	0.16	13.76	68.76	0.23	119.5
11.80	441.10	0.09	0.18	-31.88	31.80	0.27	119.5
46.48	135.37	0.18	0.17	4.84	81.63	1.44	195.1
47.19	35.53	0.17	0.17	0.00	147.34	1.67	59.4

Cont.

Q (m^3/s)	RT (s)	$WL(Tn)_2$	$WL(Tn)_1$	J(MTEMM) Bq/m^2s	J(MTMV) Bq/m^2s	v m/s	L m
10.01	519.97	0.23	0.22	3.46	79.50	0.23	119.5
13.71	37.31	0.13	0.12	9.61	98.48	0.83	30.8
16.52	41.98	0.08	0.11	-30.72	57.62	0.64	26.8
84.79	67.06	0.18	0.16	14.35	111.15	3.46	231.7
27.84	176.93	0.14	0.10	19.82	67.45	0.59	103.7
7.39	89.18	0.08	0.06	6.97	25.40	0.96	85.4
7.08	93.09	0.04	0.01	10.18	13.19	0.92	85.4
18.88	43.15	0.11	0.05	48.51	80.35	1.27	54.9
11.33	159.68	0.09	0.07	7.81	33.84	0.50	79.3
9.44	85.78	0.13	0.13	0.00	57.60	0.53	45.7
9.20	88.02	0.08	0.07	4.97	35.61	0.52	45.7
6.13	132.11	0.08	0.09	-3.96	29.23	0.35	45.7
25.96	18.83	0.09	0.09	0.00	120.98	1.20	22.56
76.92	51.33	0.57	0.48	79.92	424.54	3.03	155.5
70.50	56.00	0.37	0.36	8.32	253.73	2.78	155.5
80.13	49.27	0.36	0.39	-27.49	259.58	3.16	155.5

Notes: The symbols Q, RT, $WL(Tn)_2$, $WL(Tn)_1$, J(MTEMM), J(MTMV), v, and L stand, respectively, for airflow rate, air residence time, ^{220}Rn progeny Working Level at downstream location, ^{220}Rn progeny Working Level at upstream location, flux density according to the MTEMM model, flux density according to the MTMV model, air velocity, and distance between sampling stations.

Table 4 - Flux ratio, $J(^{220}Rn)/J(^{222}Rn)$, for several underground locations

Date YY/MM/DD	Location	$J(^{222}Rn$ (Bq/m^2 s)	$J(^{220}Rn)$ (Bq/m^2 s)	$J(^{220}Rn/J^{222}Rn)$	RT (s)
87/05/04	Shaft	2.83	5.73	2.0	193.6
86/12/11	Reef (A)	6.60	6.57	1.0	137.4
87/06/04	Reef (B)	1.46	14.76	10.1	133.5
87/04/01	Surf. ramp	0.54	7.09	13.1	430.8
87/05/25		0.38	3.71	9.8	337.9
87/01/05	Haulage	5.76	171.21	29.7	1057.4
87/01/26	way	2.64	81.56	30.9	1306.8
87/04/22		1.11	70.26	63.3	3429.6
87/03/30	Ramp in	63.47	131.10	2.1	12.5
87/04/27	waste	14.76	94.70	6.4	13.7
87/04/28		67.56	146.70	2.2	13.7
87/03/30	Ramp in	13.00	161.36	12.4	18.2
87/04/27	waste	12.05	22.17	1.89	20.0
87/04/28		9.82	44.47	4.45	19.9
87/04/08	Travelway	24.90	59.83	2.4	66.2
87/05/12		21.67	14.66	0.7	73.7
87/03/04	Airway/	38.33	83.54	2.2	42.8
87/04/20	travelway	29.07	101.16	3.5	40.9
86/12/23	Exhaustway	11.99	312.24	26.0	1241.8
87/05/14		7.82	76.45	9.8	1426.1

Note: 1. RT stands for mine air residence time.
2. A and B are two locations at an underground mine reef.

APPENDIX

There are a number of mine models that have been developed to describe the behaviour of ^{222}Rn and its progeny in underground U-mines. These models have been modified by the author to apply to mines containing thorium, and hence, mines where ^{220}Rn and its progeny are found in significant amounts[12]. For a number of reasons discussed elsewhere[8,9], only two mine models are applicable in the context of this paper, namely, the Modified Thomas-Epps Mine Model (MTEMM) and the Mine Tunnel Model with Ventilation (MTMV). The expressions used in this paper for calculating the ^{220}Rn flux density, $J(^{220}Rn)$, are given below (see also refs. 8 and 9).

1. MTEMM

The flux density for this model is given by:

$$J(^{220}Rn) = \frac{\Delta[^{220}Rn]\lambda V}{S(1-e^{-\lambda t})}$$

where, λ is the radioactive decay constant for ^{220}Rn,

$[^{220}Rn]$ is the ^{220}Rn activity concentration,

Δ stands for increment between the values determined at the two sampling stations,

V is the volume of the mine section under consideration, and

S is the surface area of the mine section under consideration.

2. MTMV

The flux density for this model is given by:

$$J(^{220}Rn) = \left[\frac{[^{220}Rn]_2 - [^{220}Rn]_1 e^{-\Lambda t}}{S(1-e^{-\Lambda t})}\right]\Lambda V$$

where, $[^{220}Rn]_2$ and $[^{220}Rn]_1$ are the ^{220}Rn activity concentrations at the downstream and upstream sampling locations, respectively.

Λ is given by: $\Lambda = \lambda+(Q/V)$, and

Q is the airflow rate.

As previously indicated $[^{220}Rn]$ is calculated from WL(Tn) or PAEC(Tn).

LIST OF FIGURES

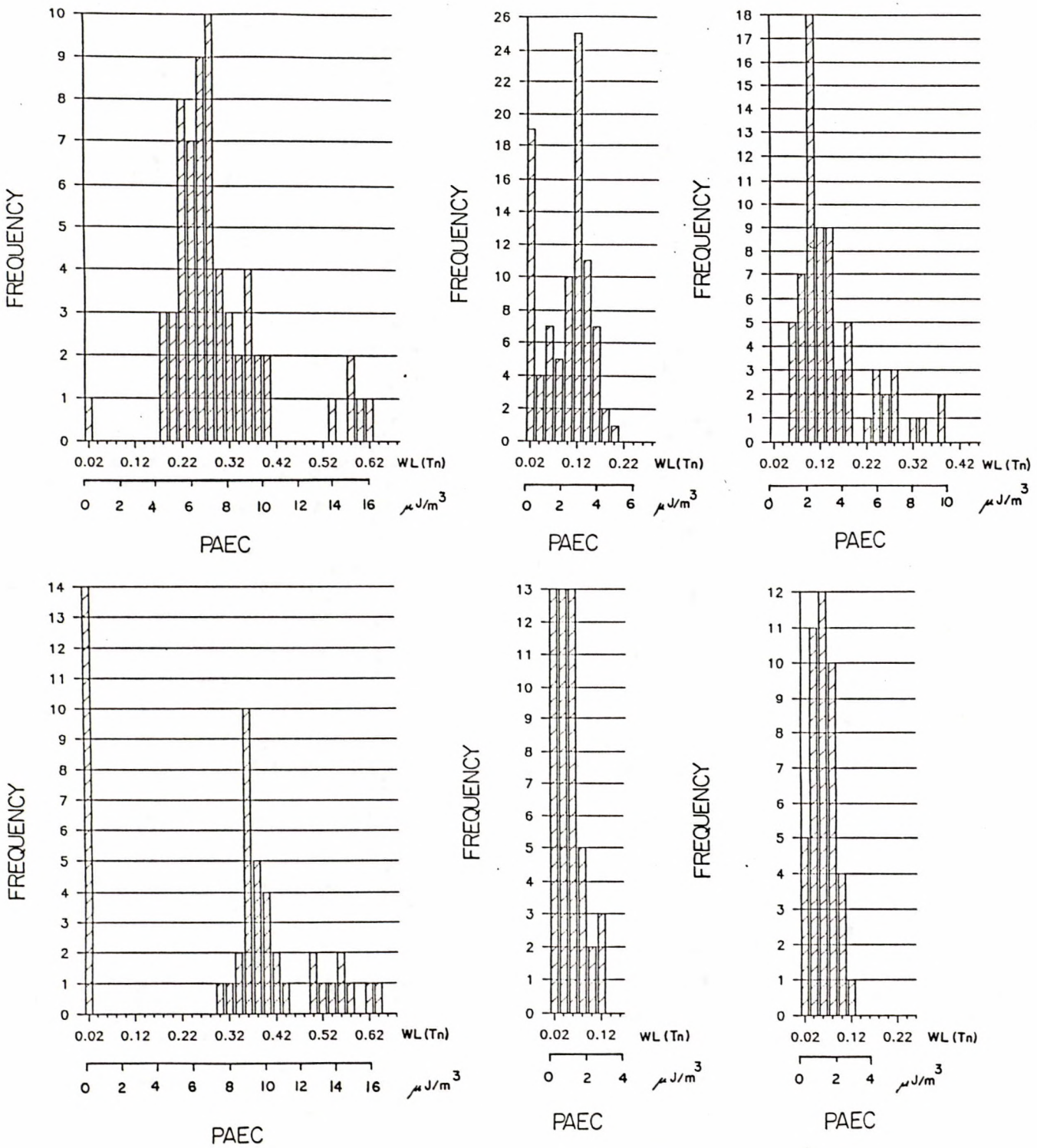
FREQUENCY
0.02 0.12 0.22 0.32 0.42 0.52 0.62 WL(Tn)
0 2 4 6 8 10 12 14 16 μJ/m3
PAEC
FREQUENCY
0.02 0.12 0.22 WL(Tn)
0 2 4 6 μJ/m3
PAEC
FREQUENCY
0.02 0.12 0.22 0.32 0.42 WL(Tn)
0 2 4 6 8 10 μJ/m3
PAEC
FREQUENCY
0.02 0.12 0.22 0.32 0.42 0.52 0.62 WL(Tn)
0 2 4 6 8 10 12 14 16 μJ/m3
PAEC
FREQUENCY
0.02 0.12 WL(Tn)
0 2 4 μJ/m3
PAEC
FREQUENCY
0.02 0.12 0.22 WL(Tn)
0 2 4 μJ/m3
PAEC

Figure 1.

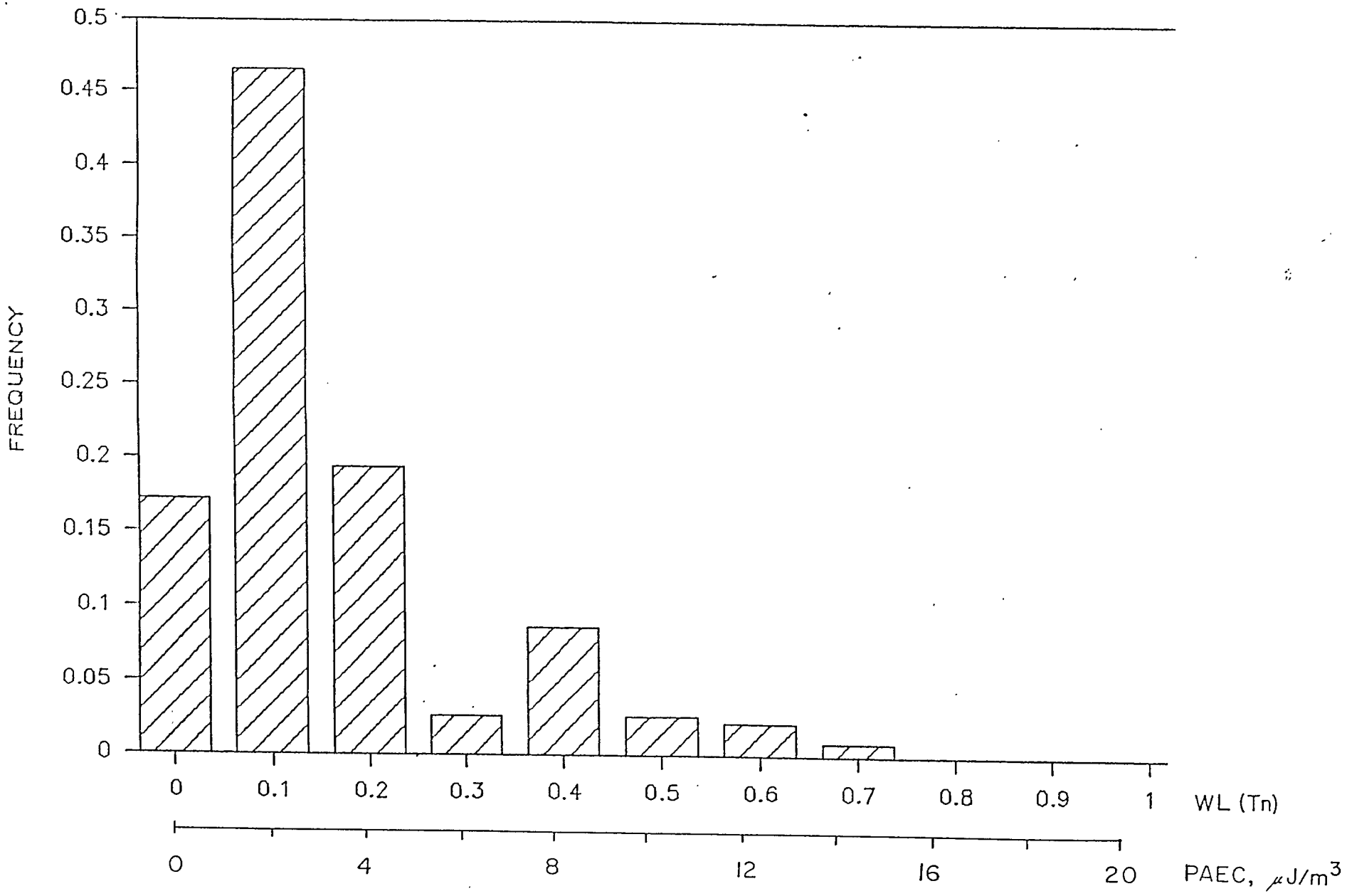
FREQUENCY
0.5
0.45
0.4
0.35
0.3
0.25
0.2
0.15
0.1
0.05
0
0
0.1
0.2
0.3
0.4
0.5
0.6
0.7
0.8
0.9
1
WL (Tn)
0
4
8
12
16
20
PAEC, μJ/m3

Figúre 2.

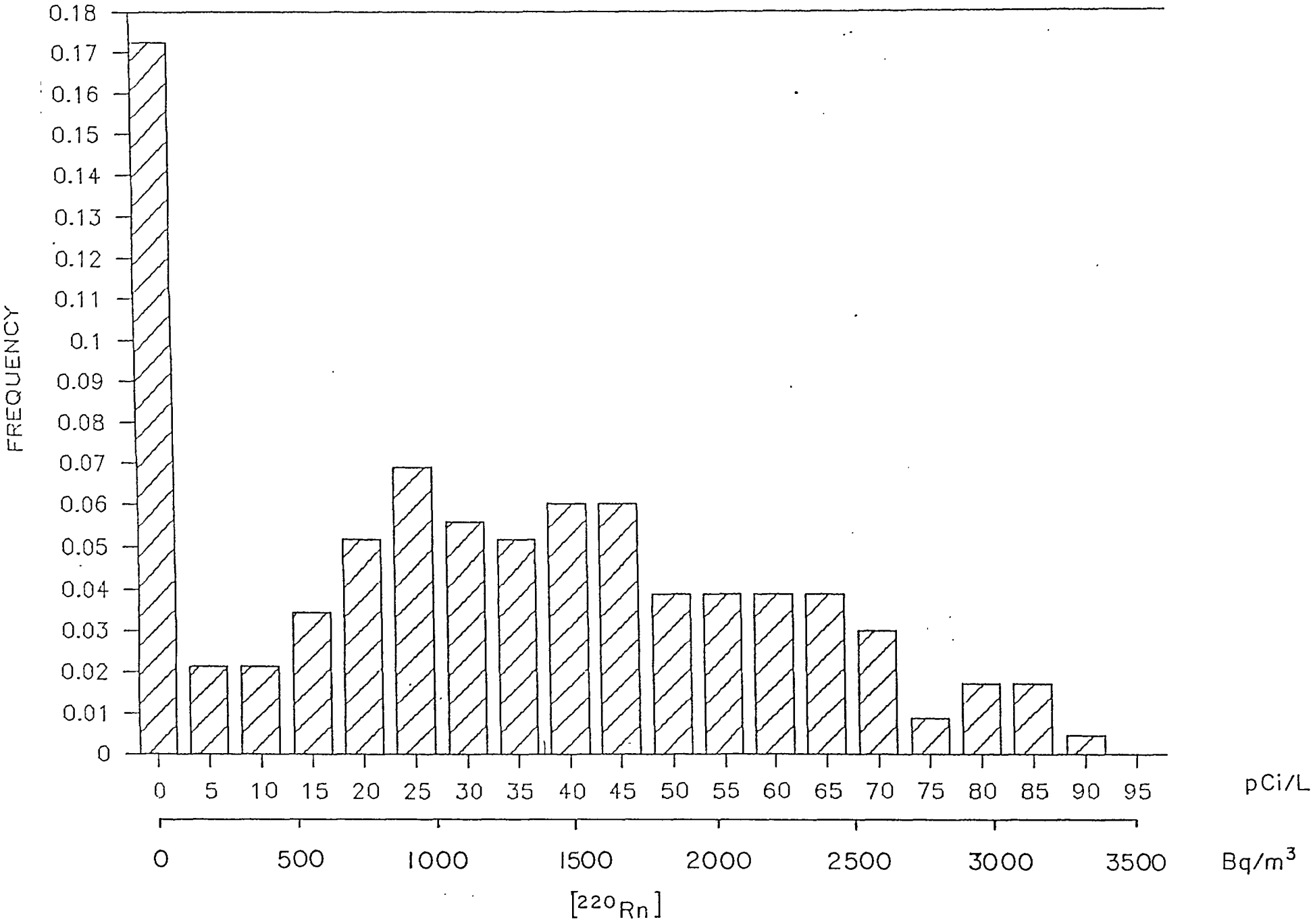
FREQUENCY
0.18
0.17
0.16
0.15
0.14
0.13
0.12
0.11
0.1
0.09
0.08
0.07
0.06
0.05
0.04
0.03
0.02
0.01
0
0 5 10 15 20 25 30 35 40 45 50 55 60 65 70 75 80 85 90 95
pCi/L
0 500 1000 1500 2000 2500 3000 3500
Bq/m3
[220Rn]

Figure 3.

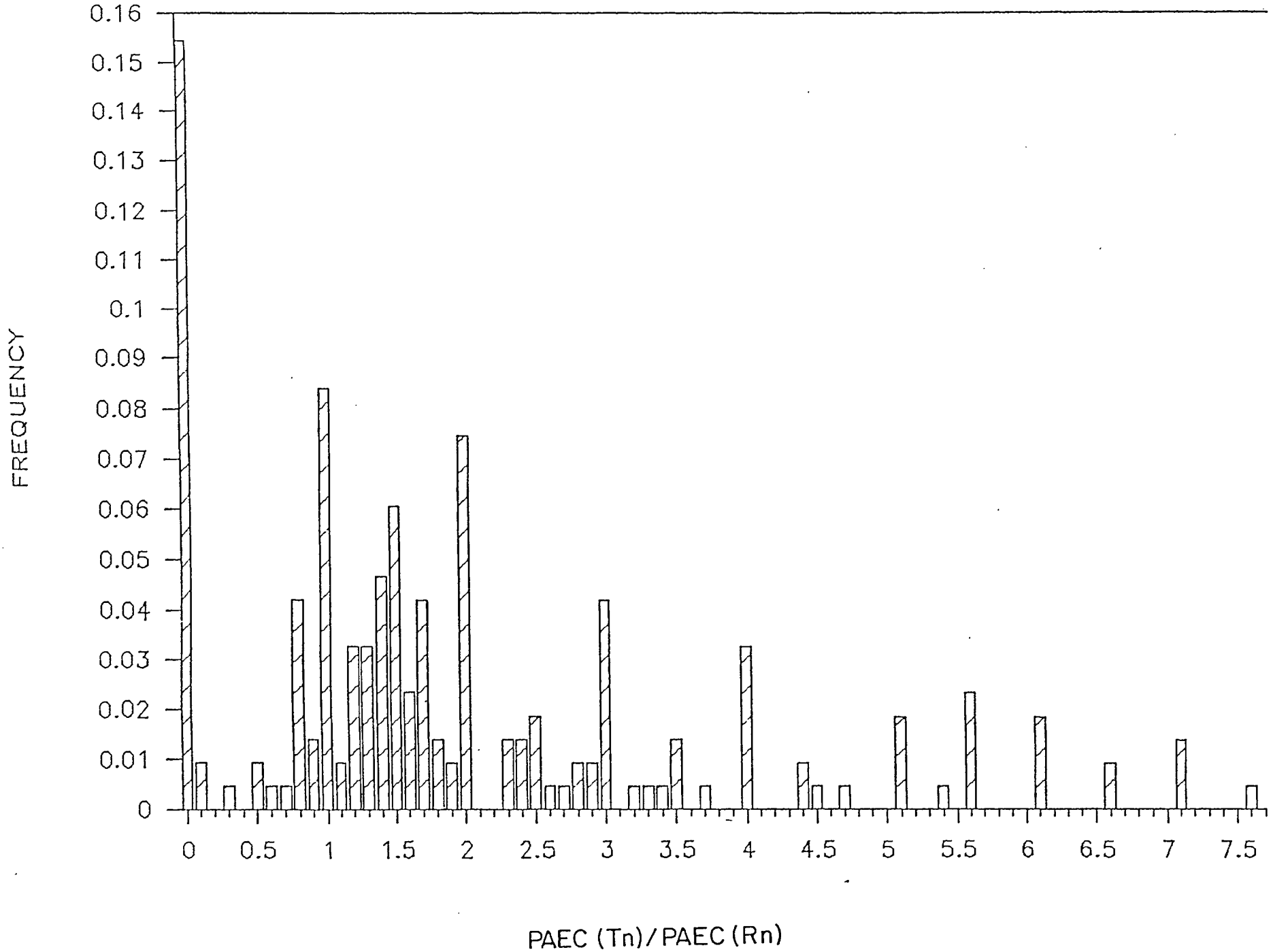
FREQUENCY
0.16
0.15
0.14
0.13
0.12
0.11
0.1
0.09
0.08
0.07
0.06
0.05
0.04
0.03
0.02
0.01
0
0
0.5
1
1.5
2
2.5
3
3.5
4
4.5
5
5.5
6
6.5
7
7.5
PAEC (Tn)/PAEC (Rn)

Figure 4.

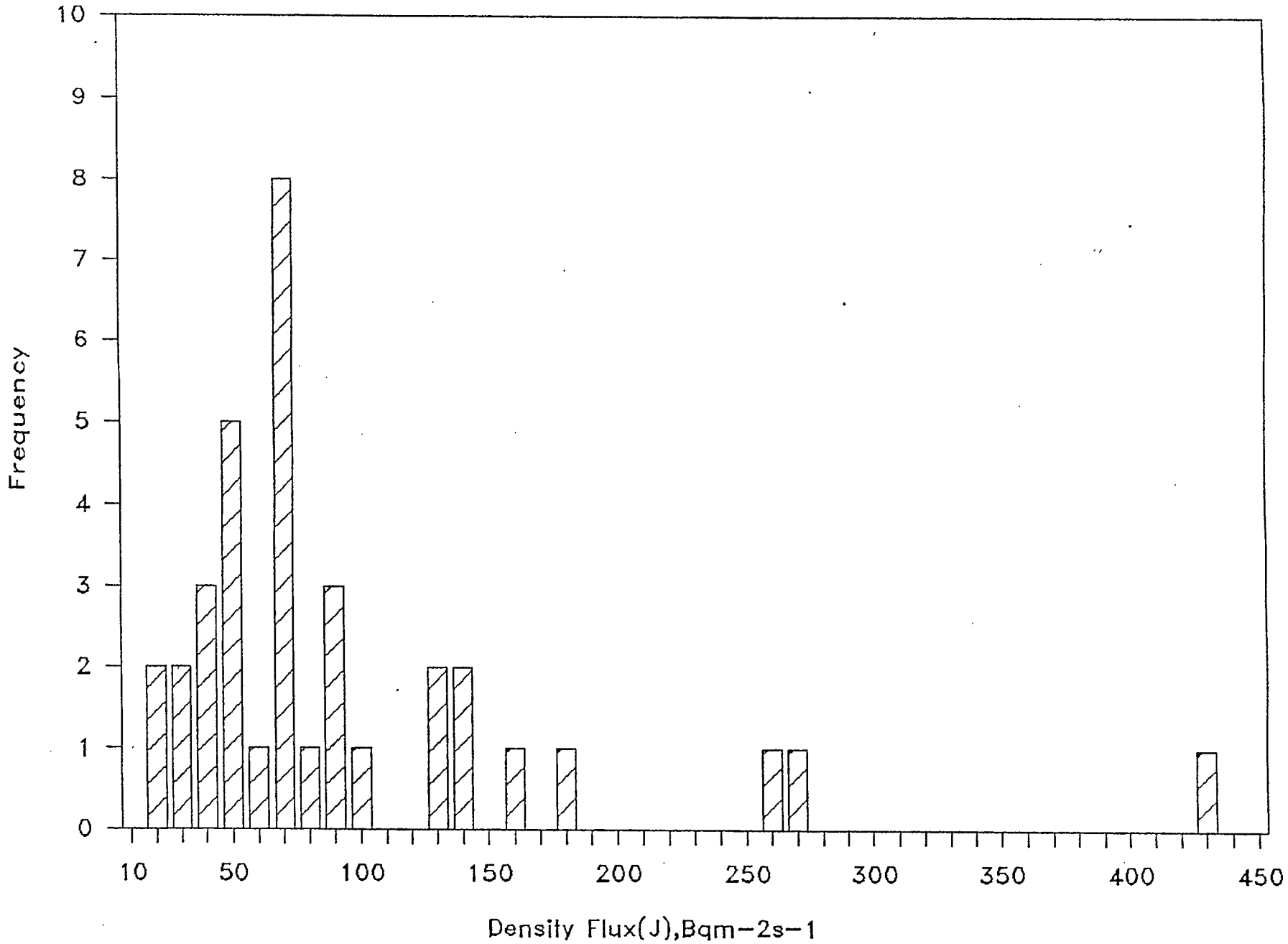
10
9
8
7
6
5
4
3
2
1
0
Frequency
10
50
100
150
200
250
300
350
400
450
Density Flux(J),Bqm−2s−1

Figure 5